SEASONAL FLUCTUATIONS IN THE ADVANCE OF A TIDEWATER GLACIER AND POTENTIAL CAUSES: HUBBARD GLACIER, ALASKA, USA

By

John Brent Ritchie

RECOMMENDED:

Advisory Committee Chair

Chair, Department of Geology and Geophysics

APPROVED:

Dean, College of Natural Science and Mathematics

Dean of the Graduate School

July 30, 2007

Date

SEASONAL FLUCTUATIONS IN THE ADVANCE OF A TIDEWATER GLACIER AND POTENTIAL CAUSES: HUBBARD GLACIER, ALASKA, USA

A

THESIS

Presented to the Faculty

of the University of Alaska Fairbanks

In Partial Fulfillment of the Requirements

for the Degree of

MASTER OF SCIENCE

By

John Brent Ritchie, B.S.

Fairbanks, Alaska

August 2007

Abstract

Satellite imagery has been used to acquire seasonal terminus positions of tidewater Hubbard Glacier, Alaska, from 1992 to 2006. During this 15 year time period the width-averaged advance of the entire terminus has been ~620 m at a mean rate of 35 m a^{-1}. Seasonal fluctuation of the terminus ranges 150 - 200 m and varies spatially. The section of the terminus near Gilbert Point exhibited little to no mean advance during this time period but displayed seasonal fluctuations of 300 - 500 m. Seasonal variability in surface ice speeds and surface seawater temperatures were also observed; both are potential forcing mechanisms for terminus fluctuations. Seasonal changes in seawater temperature of 10 to 12 °C, as well as seasonal changes in subglacial freshwater discharge are inferred to influence calving and submarine melting at the terminus, driving seasonal variations. Displacements of the medial moraine separating Hubbard Glacier and Valerie Glacier at the terminus suggest surge-like pulses of the latter with a periodicity of several years. The timing of these pulses suggests they may influence the Hubbard terminus near Gilbert Point and have implications for future closures of Russell Fjord.

Table of Contents

List of Figures

List of Other Materials

List of Appendices

Acknowledgements

I would like to thank my advisor Craig Lingle for giving me the opportunity to work on a challenging glaciological problem in some of the most beautiful country in the world. His knowledge, both within the field of glaciology and on other topics, has been a much tapped resource throughout my education. Martin Truffer suggested constructing the dataset used in this study, and his insights into tidewater glaciers were invaluable, as was Roman Motyka's working knowledge of Hubbard Glacier and tidewater glacier dynamics. Without his long-distance comments on the initial drafts of this work I would not have finished within the time frame I set for myself. I also thank Keith Echelmeyer for his insightful suggestions on this manuscript and his warm demeanor in the office. I thank Anthony Arendt and Sandra Zirnheld for teaching me to use the GIS software which was an integral part of this work; Will Harrison and Chris Larsen, both friendly faces who never turned down requests for help; and Rudi Gens and Anupma Prakash, who provided expert advice and assistance with processing and analysis of satellite imagery.

A very special thanks goes to Paul Claus and his family at Ultima Thule Lodge, Alaska. Throughout my work on the Geophysical Institute's airborne glacier laser altimetry program Paul's expert flying always caused me to feel I was in good hands. He and his family were exceptionally hospitable each and every time I was fortunate enough to visit their remote lodge from which we staged our glacier flights.

I would also like to thank all of the wonderful friends I made in Fairbanks. Whether enjoying a fire, picking some bluegrass, or playing hockey, the experiences I shared with them all are the reason Fairbanks will always have a special place in my memories.

Emily deserves a huge thanks for giving me a reason to go to Alaska and study glaciology. It is because of everything she is and does that I was lured to Fairbanks and for that I will remain eternally grateful. Without her and the life we made in our little cabin, I would not have made it through my time at UAF.

Chapter 1

Introduction

The mechanisms involved in tidewater glacier dynamics and tidewater calving remain among the largest mysteries in the field of glaciology. Understanding tidewater glaciers is an important piece to the puzzle of understanding sea level fluctuations. Additionally, calving is an important component of mass loss at ice sheets and can be a significant threat to ocean shipping lanes. The position of a tidewater glacier terminus is controlled by ice flow into the terminus and the calving rate. Seasonal fluctuations of terminus position, exhibited by tidewater glaciers, must reflect variation in either one of these two factors or a combination of both.

This study used satellite imagery of Hubbard Glacier to examine seasonal fluctuations at the terminus in order to better understand tidewater glacier dynamics and calving. Understanding the dynamics of Hubbard Glacier is of particular importance as it has a history of blocking the entrance to Russell Fjord. Future closures, if permanent, would likely have adverse economic consequences for the nearby community of Yakutat. The main chapter of this thesis (Chapter 2) is to be submitted to the Journal of Glaciology and will be co-authored with Craig Lingle, Roman Motyka, and Martin Truffer.

Two appendices have been included to supplement this manuscript. Appendix A is a table of the images used in this study, their dates of acquisition, and their type. A detailed version of the methods used in this study was written so that future work may continue and is included in Appendix B. A supplemental DVD is also included which contains files of terminus and medial moraine positions, additional files used for processing, and spreadsheets containing the results.

Chapter 2

Seasonal Fluctuations in the Advance of a Tidewater Glacier and Potential Causes: Hubbard Glacier, Alaska, USA[1]

ABSTRACT

Satellite imagery has been used to acquire seasonal terminus positions of tidewater Hubbard Glacier, Alaska, from 1992 to 2006. During this 15 year time period the width-averaged advance of the entire terminus has been ~620 m at a mean rate of 35 m a^{-1}. Seasonal fluctuation of the terminus ranges 150 - 200 m and varies spatially. A section of the terminus, near a narrow gap where the glacier has now twice closed off 40 km long Russell Fjord, exhibited little to no mean advance during this time period but displayed seasonal fluctuations of 300 - 500 m. Seasonal variability in surface ice speeds and surface seawater temperatures were also observed; both are potential forcing mechanisms for terminus fluctuations. Seasonal changes in seawater temperature of 10 to 12 °C, as well as seasonal changes in subglacial freshwater discharge are inferred to influence calving and submarine melting at the terminus, driving seasonal variations. Displacements of the medial moraine separating Hubbard Glacier and Valerie Glacier at the terminus suggest surge-like pulses of the latter with a periodicity of several years. The timing of these pulses suggests they may influence the Hubbard terminus near Gilbert Point and have implications for future closures of Russell Fjord.

---

[1] Ritchie, J.B., C.S. Lingle, R.J. Motyka, and M. Truffer, to be submitted to the Journal of Glaciology.

2.1 INTRODUCTION

The unique, dynamic behavior of tidewater glaciers is strongly influenced by calving of ice at the terminus. The rate of advance or retreat of the terminus is

$$\frac{dL}{dt} = \bar{v}_s - \bar{v}_c \tag{2.1}$$

where L is the length of the glacier, $\bar{v}_s$ is the width averaged ice speed at the terminus, and $\bar{v}_c$ is the width averaged calving speed at the terminus. In terms of water equivalent volume fluxes, Eqn. (2.1) can be expressed

$$Q_t = Q_{in} - Q_c \tag{2.2}$$

where Q_t is the rate at which ice volume is added or lost at the terminus, Q_{in} is the ice flux into the terminus, and Q_c is the calving flux (including ice loss caused by both iceberg calving and submarine melting) (O'Neel and others, 2003). Many studies have been conducted in order to understand the dynamics of tidewater glaciers (e.g.; Clarke, 1987; Krimmel and Vaughn, 1987; Meier and Post, 1987; Meier and others, 1994; O'Neel and others, 2001), particularly tidewater calving (e.g.; Brown and others, 1982; Pelto and Warren, 1991; Warren and others, 1995; Van der Veen, 1996; 2002; O'Neel and others, 2003; Motyka and others, 2003). Debate continues however, regarding the factors influencing calving and tidewater glacier dynamics. Calving can remove large amounts of ice from glaciers and ice sheets in relatively short times, particularly during catastrophic retreats. For example, Krimmel (2001) documented calving rates as high as 20 million m^3 d^{-1} at Columbia Glacier, Alaska. The rapid disintegration of the northern hemisphere Pleistocene ice sheets appears to have been caused by calving into pro-glacial lakes as well as by rapid calving retreat of ice streams grounded below sea level (e.g., Mickelson and others, 1981; Pollard, 1984; Van der Veen, 1999). A significant portion of mass loss from both the Greenland ice sheet (about 56%; Reeh, 1994) and the Antarctic ice sheet (about 77%; Jacobs and others, 1992) is due to calving from outlet glaciers having both floating and grounded termini. Also, all of the recently reported rapid changes in Greenland are due to increased calving (e.g., Rignot and Kanagaratnam, 2006).

Previous studies of grounded tidewater glaciers have shown that annually-averaged calving rates are correlated with water depth at the calving front (Brown and others, 1982; Pelto and Warren, 1991). Additional studies have shown that this correlation does not hold on a seasonal or shorter time scale (Sikonia, 1982; Van der Veen, 1996; Motyka and others, 2003). Sikonia (1982) argued for a correlation between water discharge at the bed and seasonal calving rates. All these relationships are empirical. A study of LeConte Glacier by Motyka and others (2003) showed that submarine melting can be an important seasonal contribution to ice loss at the face of tidewater glaciers. The controlling factors

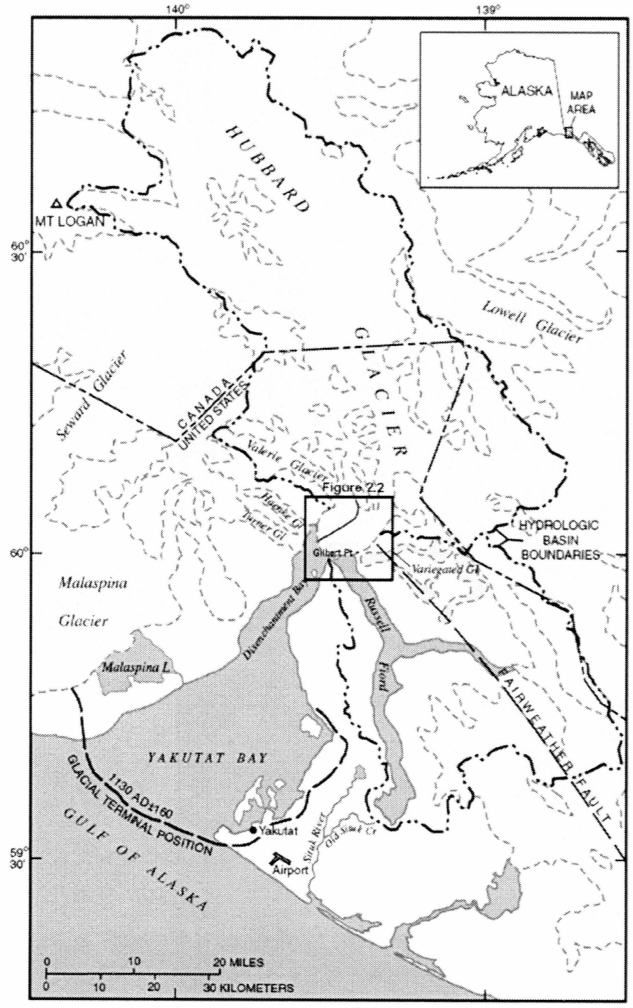

Figure 2.1. Map of Hubbard Glacier showing maximum glacial extent in the early 1100's (modified from Trabant and others, 2003). The terminus is composed of ice from Hubbard and Valerie Glaciers, separated by a medial moraine.

are forced convection at the ice-water interface driven by subglacial discharge of freshwater and the influx of warm saline water. Van der Veen (2002) suggested that the terminus position is maintained by the height of the ice face above flotation. In this model, the calving rate is determined by both glacier speed and thickness change at the terminus. Given these ideas, the factors influencing calving rate appear to be a complex combination of many factors. Given that dL/dt is between one and two orders of magnitude smaller than either the ice velocity or the calving rate, it seems clear that these two cannot be entirely independent of each other (Eqn. 2.1).

Tidewater glaciers have been shown to exhibit seasonal variations in their terminus positions (Meier and Post, 1987; Sohn and others, 1998; Krimmel, 2001; Motyka and others, 2003). Eqns. (2.1) and (2.2) indicate that this must reflect seasonal variations in ice speed at the terminus, calving rate, or a combination of the two. Here we document similar seasonal oscillations in terminus position at Hubbard Glacier (Fig. 2.1), Alaska, using satellite images that span the years 1992 - 2006. We present our data and explore the factors that may be influencing these variations as well as the stability of the terminus. In addition, we examine displacements of the medial moraine separating Hubbard Glacier and Valerie Glacier at the terminus (Fig. 2.1), and sea surface temperatures within the main area of Yakutat Bay and adjacent Gulf of Alaska (GOA). It is thought that water temperatures affect calving of tidewater glaciers (e.g.; Walters and others, 1988; Motyka and others, 2003). We investigate this by looking for possible relationships between changes in terminus position and sea surface temperatures.

2.2 HUBBARD GLACIER

Hubbard Glacier, with an area of 2450 km^2 (Arendt and others, 2002), is the largest non-polar tidewater glacier in the world. It descends over 120 km from its origins, on the flanks of Mount Logan (5959 m) in Yukon, Canada, to sea level where it terminates in Disenchantment Bay and Russell Fjord near Yakutat, Alaska (Fig. 2.1). The height of the calving face ranges from 60 - 100 m a.s.l. and has a curvilinear width of 11.5 km. On the

western side of the terminus the first 2 km is composed of ice originating from Valerie Glacier (Fig. 2.1).

Hubbard Glacier has historically revealed behavior that is asynchronous with regional glacier trends and seemingly independent of climate. Moraine deposits at the seaward entrance to Yakutat Bay (Fig. 2.1) have indicated that the glacier filled the entire bay as recently as AD 1100 (Plafker and Miller, 1958; Barclay and others, 2001). Water depths along this moraine average about 15 m and are nowhere deeper than 30 m. Barclay and others (2001) showed retreat was underway by AD 1380 and the records of A. Malaspina in 1792 and G. Vancouver in 1794 suggest that the head of the glacier was well into Disenchantment Bay by 1791 (Fig. 2.1). This implies a 410 year retreat during the Little Ice Age averaging 130 m a^{-1}. This was a time when other glaciers throughout Alaska and NW North America were advancing (Porter, 1989; Motyka and Beget, 1996; Wiles and others, 1999). Since first being mapped in 1895 by the International Boundary Commission, the glacier has advanced over 2.5 km (Davidson, 1903; Trabant and others, 2003). This is in direct contrast to the regional trend: glaciers throughout Alaska and adjacent Canada have been retreating, some rapidly, during the past century (Arendt and others, 2002; Larsen and others, 2007).

Hubbard Glacier has a history of blocking the seaward entrance to Russell Fjord, which has a relatively large freshwater catchment area, thus creating a glacier-dammed lake (Fig. 2.1). Barclay and others (2001) showed that three major Holocene expansions of Hubbard Glacier have blocked Russell Fjord early in each advance. Twice in recent history the glacier has temporarily blocked the entrance to Russell Fjord; on both occasions the dam failed catastrophically (Motyka and Truffer, 2007). In April and May of 1986 an emergent push moraine appeared at the terminus near the entrance to Russell Fjord, causing calving to stop. Mayo (1988; 1989) recorded a velocity of 36 m d^{-1} in June of 1986 on Valerie Glacier near its junction with Hubbard. Combined with observations of wrench faulting and mud and silty water being extruded from the terminus, this high velocity led Mayo to conclude that a surge of Valerie Glacier had occurred. Shallow waters near Gilbert Point facilitated the forward movement of a finger of ice which

created an ice and push-moraine dam in May of 1986. The subsequent dam failure and lake outburst in October of 1986 eroded the sediments near Gilbert Point to depths of 35 m or more (Trabant and others, 1991, Cowen and others, 1996). A 1999 NOAA bathymetric survey showed that water depth averaged 25 m near Gilbert Point, suggesting a sediment infill in this area. In June of 2002 an ice and push-moraine dam once again closed the entrance to Russell Fjord (Trabant and others, 2003; Motyka and Truffer, 2007). Heavy rain in August, 2002 caused Russell Fjord to overtop the moraine dam and rapid erosion resulted in dam failure accompanied by an outburst flood. The possibility of a sustained closure of Russell Fjord is of concern to Yakutat residents as it may result in negative consequences for the Situk River, an important economic resource.

Hubbard Glacier is considered to be in the advance phase of the so-called tidewater glacier cycle (Post, 1975; Meier and Post, 1987; Post and Motyka, 1995; Trabant and others, 2003). The tidewater glacier cycle describes the cyclic behavior of slow advance and rapid retreat exhibited by calving glaciers grounded below sea level in fjords. Advancing calving glaciers, driven by a high accumulation to total area ratio (AAR), advance into fjords by remobilizing subglacial sediments and by slowly pushing forward their terminal moraine shoals down-fjord (Hunter and Powell, 1998; Motyka and others, 2006). The typical advance rate for this process is a few meters to tens of meters per year. If, for any reason, the terminus retreats from its terminal moraine shoal into deeper waters, an irreversible retreat can be initiated. This can occur when the glacier reaches mass-flux equilibrium at an AAR of approximately 0.7 (Post and Motyka, 1995; Trabant and others, 2003). Van der Veen (2002) suggests that thinning at the terminus of a tidewater glacier may also cause initiation of retreat. The rate at which a calving glacier retreats is typically on the order of 100 - 1000 m a^{-1} (Meier and Post, 1987). Retreat then continues until the glacier terminus reaches a stable position, typically at a neck in the fjord or at the inland end of the fjord where the fjord bottom rises above sea level. Tidewater glacier retreat is often catastrophic, which rapidly increases the AAR resulting in sufficient ice flux to once again advance the glacier. The remobilization of soft sediments, to create and maintain a terminal moraine, has been shown to excavate deep

basins to well below sea level which serves to accelerate calving during retreat (Motyka and others, 2006). A tidewater glacier can take many centuries to 1000 years to advance to the seaward end of its fjord (Meier and Post, 1987), but can retreat the same distance back up its fjord in only a few decades once stability from its moraine shoal is lost.

2.3 METHODS

2.3.1 Image Processing

Seasonal terminus positions of Hubbard Glacier were derived from satellite images for the period 1992 through 2006. The primary source for this dataset was synthetic aperture radar (SAR) images obtained from the Alaska Satellite Facility (ASF) at the University of Alaska Fairbanks. We have used images from the European Space Agency's ERS-1 and ERS-2 satellites, and the Canadian Space Agency's RADARSAT-1 satellite. In a few cases, images were also obtained from NASA and the U. S. Geological Survey's (USGS) Enhanced Thematic Mapper Plus (ETM+) instrument onboard the Landsat 7 satellite. One image was also obtained from NASA's Advanced Spaceborne Thermal Emission and Reflection Radiometer (ASTER). We use radar imagery for its ability to record an image regardless of time of day and cloud cover which is especially useful in coastal SE Alaska where it is rarely clear. We have used standard beam SAR images which have 12.5 m pixel spacing. The resolution is similar for the Landsat images and the ASTER image which both have 15 m pixel spacing. An important characteristic of RADARSAT imaging which makes it suitable for this study, is its 24 day repeat orbit. Since the area of interest (the region near the terminus of Hubbard Glacier) is small (270 km^2) compared to the image footprint (10000 km^2), an exact repeat is not needed to capture the desired region. Our primary concern was to obtain images from roughly the same date each year as opposed to obtaining exact repeat images.

Every image used in this study has been properly geocoded and coregistered in order to be compared within the same reference frame. Using ASF's Convert tool (http://www.asf.alaska.edu/softwaretools/convert/), the images were geocoded to a Universal Transverse Mercator (UTM) projection using the World Geographic System

(WGS) datum of 1984. Upon close inspection it was discovered that about 20 images were improperly coregistered and randomly shifted by 10 to 100 m. These images were coregistered by hand using Gilbert Point as a reference (Fig. 2.2). The Landsat images and the ASTER image were geocoded to the same datum and then coregistered by hand using the same technique.

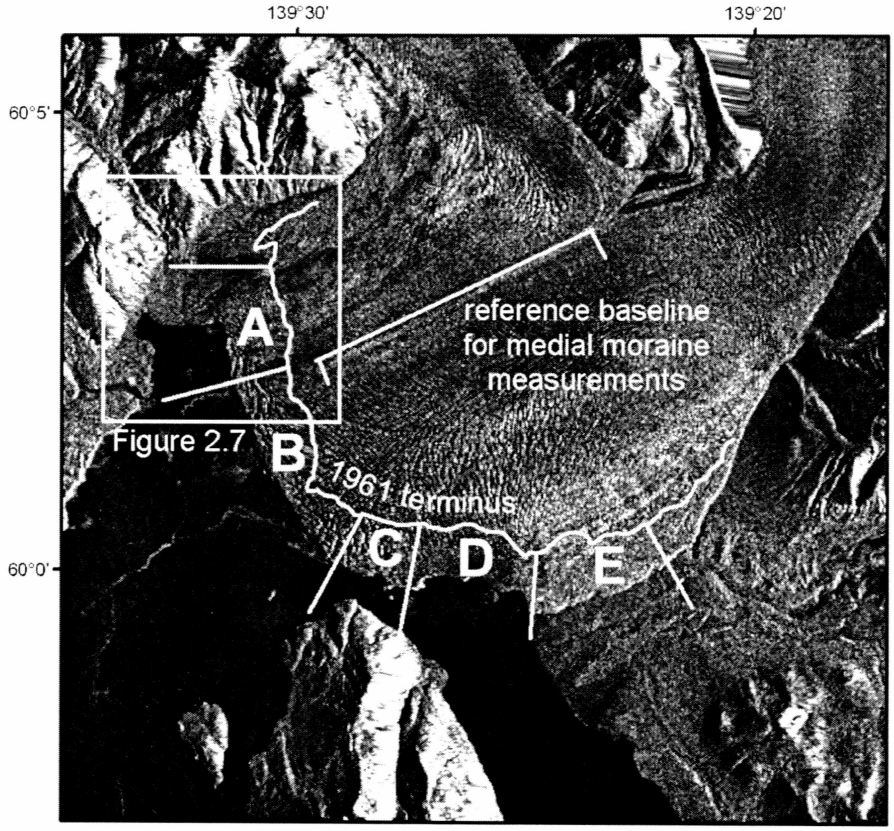

Figure 2.2. The terminus of Hubbard Glacier is separated into 5 sections based on contributing factors to terminus position. The location of Figure 2.7 is also shown, along with the reference baseline used to measure medial moraine displacement. © CSA 2003.

2.3.2 Image Analysis

We acquired a set of 59 separate terminus positions of Hubbard Glacier, spanning the period 1992 through 2006. The images were selected in order to establish a seasonal cycle. We limited our analysis to 4 images per year, which is sufficient to satisfy the Nyquist criteria for annual cycles. Ideally these positions would be taken in late January, early May, late July, and mid October. Since the 24 day repeat cycle of SAR satellites

does not result in repeat images on the same date each year, it was not always feasible to obtain images at the same time each year. Therefore images were obtained as close to these dates as possible. Also, there are large data gaps, most importantly between December of 2001 and September of 2002. This gap is important because it spans the 2002 closure of Russell Fjord.

The terminus of Hubbard Glacier was divided into 5 sections, each of which can be distinguished by a different set of influencing factors (Fig. 2.2). Section A is made up of ice that flows from Valerie Glacier as defined by the medial moraine separating Valerie from the main branch of Hubbard Glacier. Here the terminus not only calves into Disenchantment Bay, but it also terminates on a mudflat. Section B is defined as ice flowing down from the main branch of the Hubbard Glacier and terminating into the waters of Disenchantment Bay. The third section, Section C, is defined by its vicinity to Gilbert Point. To the east, Section D calves into the waters of Russell Fjord. At the eastern end of the terminus, the land terminating Section E is advancing over glacier outwash deposits of the nearby Variegated Glacier. Examining the behavior of each of these terminus sections separately is important for understanding variations of terminus position.

The location of the terminus was digitized in each of the satellite images. This was performed at approximately a 1:9,000 scale. The 1961 location of the terminus was determined from USGS maps, which were made from aerial photographs (Fig. 2.2). This location provided a baseline for comparing the terminus positions acquired from the satellite images. The areas in each of the five polygons defined by the 1961 baseline, satellite terminus positions, and divisions between sections were measured on each image (Fig. 2.2). In order to compare one section to another, the changes in area were converted to average linear changes. Dividing the area of each polygon by its width resulted in a measurement of length which represents the total change in length since 1961 averaged over the entire section. Using the furthest east and west boundary lines, we similarly came up with a polygon and resulting change in length since 1961 averaged over the entire terminus. An additional terminus position was estimated for the Gilbert Point

section (section C) for July, 2002 using an aerial photograph taken by the National Marine Fisheries Service (NMFS) during the closure of Russell Fjord. Using the photograph as reference, the terminus position was estimated and digitized in the same reference frame as the satellite images and processed in the same manner. It is important to note that we have used a constant width which we feel is representative for each section. Since the dividing lines are not parallel to each other, the width used does not reflect the non-constant width of each section. Therefore, the average linear change has relative but not absolute meaning, and should not be compared to similar data obtained by a different method.

2.3.3 Assessment of Medial Moraine Displacement

We also used the satellite images to examine fluctuations of the moraine which separates the Valerie from the Hubbard Glacier. Due to snowfall covering the glacier, only the images taken in summer or fall showed this moraine clearly. We digitized the position of the moraine for all images in which it was distinguishable, which was typically only once per year. An arbitrary baseline was used as a reference (Fig. 2.2). Using the same technique used for the terminus change data, the moraine positions were combined with the reference baseline to determine areas with which to obtain width-averaged values of linear offset. In this manner, a time series of medial moraine movement was constructed. This dataset helps to establish the flow relationship between Valerie Glacier and the main branch of the Hubbard Glacier.

2.3.4 Error Assessment of Image Derived Data

The method we used for terminus digitization is somewhat subjective. Two sources of uncertainty arise form this process: 1) the error associated with the coregistration process, and 2) the uncertainty in terminus digitization. Because this region is highly glaciated and landscapes are constantly changing, the satellite images do not contain many features that can be confidently recognized from one image to another to use for coregistration. The region is also sparsely populated and manmade features are not abundant. One feature

that is easily distinguishable and visible on most of the images is the intersection of two runways at the Yakutat airport. We determined the coordinates of this location for 14 images and obtained a standard deviation of 18 m and 15 m for x and y respectively. The effect on the terminus of shifting an image along the x-direction as opposed to the y-direction depends on the terminus orientation. To simplify, we have used the maximum possible error of 23 m.

The next source of error is the uncertainty in determining the terminus boundary. This uncertainty involves not only the pixel size of the image, but also the ability of an operator to effectively determine this boundary. We used two different methods to assess this error, both of which involve the repeatability of determining width-averaged change in length. For each of 10 images, we repeated the terminus digitization process and in doing so obtained two distinct values of average linear change for each image. The standard deviation of the differences between these two values for the 10 images is 9 m. The second method involved taking one image, repeating terminus digitization 10 times, and processing these repeat digitizations to obtain an average linear change. The standard deviation of these average linear change values was 7 m. Since these two methods assess the same source of error, we have chosen the higher of these two values to represent this error. Whether or not an image is shifted does not affect the determination of the terminus boundary, and therefore these two sources of error are independent. By error propagation, the overall uncertainty for image derived datum is ± 25 m.

2.3.5 Sea Surface Temperature

Some studies have indicated that ocean temperatures can affect the seasonal and perhaps the long-term stability of TWG termini (e.g.; Walters and others, 1988; Motyka and others, 2003). Only sporadic temperature measurements are available within Disenchantment Bay (Motyka and Truffer, 2007). The best long term temperature records are from satellite sea surface temperatures. We use these measurements as a proxy for water temperatures. We obtained spatially averaged, monthly sea surface temperature (SST) records from NASA's Physical Oceanography Distributed Active Archive Center

(PO.DAAC), which are derived from the 5-channel Advanced Very High Resolution Radiometers (AVHRR) on board NOAA's polar orbiting satellites. We have used the Pathfinder Version 5.0 SST monthly data, which is a reanalysis of the AVHRR data stream developed by the University of Miami's Rosenstiel School of Marine and Atmospheric Science (RSMAS) and the NOAA National Oceanographic Data Center (NODC). This reanalysis allows for an improved 4 km resolution and has an accuracy of 0.5° C. Each monthly temperature record is the spatial average of temperatures derived within Yakutat Bay and the GOA. Reanalysis of the data stream results in a time lag between data acquisition and distribution. As a result, we were only able to obtain SST data up to 2004.

2.4 RESULTS

2.4.1 Terminus Change

The results from the terminus position analyses are shown in Figure 2.3. The width averaged change in terminus position since 1961 is given for each of the 5 sections (Fig. 2.3a-e) along with the change averaged over the entire terminus (Fig. 2.3f). The open circles represent the fall position for each year and help define the seasonal multi-year trend. The data gap in 2002 is a reflection of the lack of imagery at that time. The terminus position for Gilbert Point derived from the NMFS aerial photograph is represented by a dotted line in Figure 2.3c.

The section of the terminus consisting of ice from Valerie Glacier (Fig. 2.3a) shows a period of slow advance from 1992 to 2000 at an average rate of 28 m a^{-1}. This is followed by 2 years of accelerated advance which averages 268 m a^{-1} and then an average advance rate of approximately 0 m a^{-1} from 2002 through 2006. Throughout all of these time periods there exists a seasonal signal averaging around 100 m.

Section B, which is bounded by Disenchantment Bay, shows fairly regular behavior consisting of winter advance followed by summer retreat (Fig. 2.3b). Superimposed on an average advance rate of 42 m a^{-1} are seasonal fluctuations averaging 175 m. Retreats of up to 250 m occur over the time span of only 2-3 months in late summer. Examination of

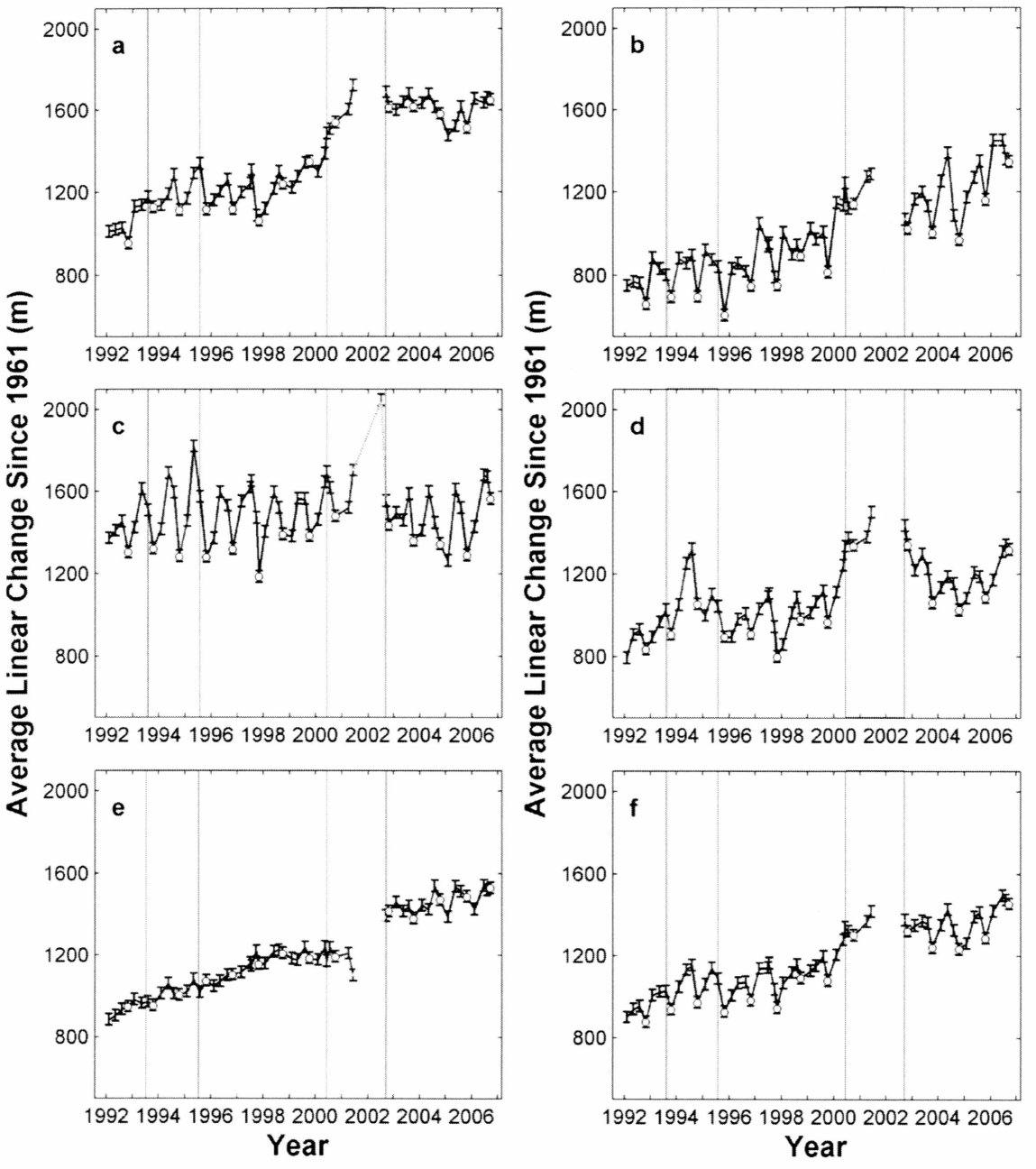

Figure 2.3. Average linear change (with associated error) for the 5 sections of Hubbard Glacier: a) Valerie Glacier ice, b) Disenchantment Bay, c) Gilbert Point, d) Russell Fjord, e) eastern land-based ice, and f) the entire terminus. Circles represent fall position. Dotted line in section C represents estimate of 2002 position from aerial photography. Shaded bars depict timing of medial moraine displacement events.

images revealed that large embayments, 100 - 500 m in radius, form on average about 50% of the summers.

The seasonal fluctuations seen near Gilbert Point are the most dramatic (Fig. 2.3c). These fluctuations average 300 m and can be larger than 500 m in one year. Large seasonal changes in terminus position are superimposed over an average advance rate of only 5 m a^{-1}. The absence of any long term advance rate coupled with relatively large seasonal fluctuations sets this region apart from the rest of the terminus.

The section of the terminus bounded by Russell Fjord exhibits the most erratic behavior of all the sections (Fig. 2.3d). While the 2006 position is further advanced than the 1992 position, this section fluctuated from advancing to retreating modes on time scales of several years. Large advances occurred in 1993-94 and 1999-2000 at rates of 520 m a^{-1}. These large scale advances were followed shortly by retreats of similar magnitude. Examination of Figure 2.2 shows that this section has a unique geometry with a bay-like appearance. During these periods of accelerated advance and retreat, the change in terminus position occurs almost exclusively in the western end of this section, closest to Gilbert Point.

The land based section of the terminus shows no signs of seasonal fluctuation (Fig. 2.3e) and has been advancing at a uniform rate of 43 m a^{-1}.

The change in position for the entire terminus (Fig. 2.3f) over the time period of this study is remarkably uniform. An examination of the 5 individual sections of the terminus might lead one to predict that the trend for the entire terminus should be complicated. However, it appears that the somewhat erratic behavior in some of the individual sections cancels out when integrated across the terminus, resulting in an almost uniform advance of the entire terminal face with a steady seasonal signal superimposed. The terminus advances throughout the winter and reaches its furthest extent by spring. It then undergoes retreat during the summer, and by fall the most retracted position is attained. During a typical year the average position of the terminus fluctuates by 125 m. This seasonal cycle is consistent for the entire interval of this study, with the overall trend being slow advance. Throughout this period the terminus has advanced approximately

620 m at an average rate of 35 m a^{-1}. Since 1961 the entire terminus has advanced an average length of 1495 m which reflects a similar average advance rate of 33 m a^{-1}.

2.4.2 Medial Moraine Displacement

Examination of the medial moraine separating Hubbard Glacier from Valerie Glacier (Fig. 2.2) revealed two distinct displacement events during the time period of this study (Fig. 2.4). From August 1993 to August 1995, the moraine was offset, on average, 100 m to the southeast. Over the next 4 years the moraine shifted back to the northwest and by August of 1999 it had returned to roughly the same configuration that it occupied in 1992. A second displacement, averaging 280 m, occurred between July 2000 and September 2002. This large offset to the southeast is followed by a similar, but opposite, offset to the northwest over the following 4 years.

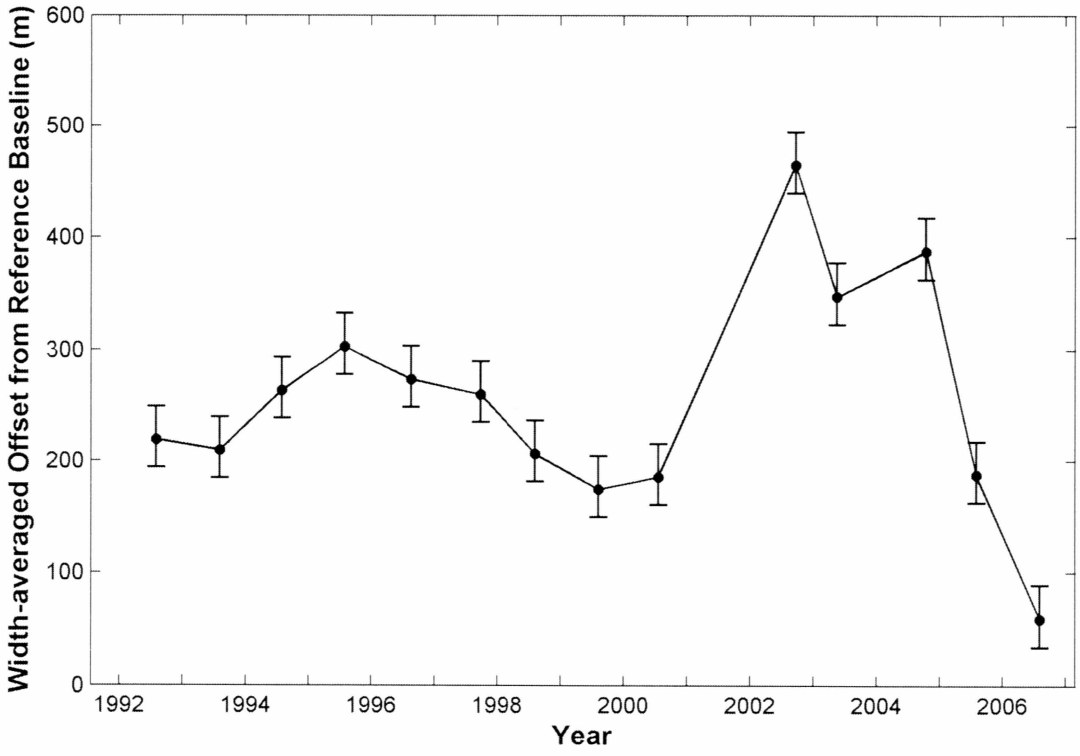

Figure 2.4. Time series of medial moraine offset relative to an arbitrary reference baseline. Values of offset are averaged over the length of the baseline.

2.4.3 Sea Surface Temperature Record

The spatially averaged, monthly mean sea surface temperature record is shown in Figure 2.5. The seasonal variability in temperature ranges from 10 - 12 °C. Typically the coldest temperatures occur during December, January, February, and March with little variability during these months. By contrast, the warmest temperatures are seen in July, August, and September, but the variability in summer temperatures can be as high as 4 °C.

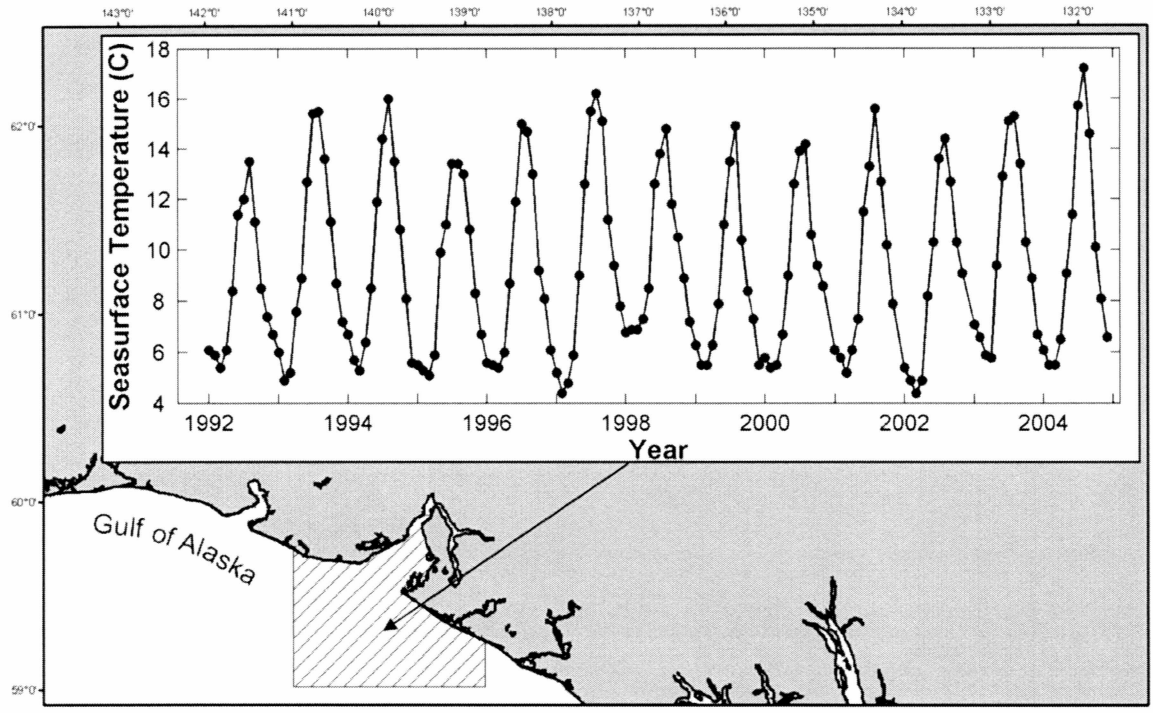

Figure 2.5. Monthly mean sea surface temperatures which are spatially averaged over the shaded area within Yakutat Bay and extending into the Gulf of Alaska.

2.5 DISCUSSION

2.5.1 Interpretation of Medial Moraine Movement

We interpret the displacement events seen in the medial moraine as representing an increase in the flow of ice of Valerie Glacier. Valerie Glacier has been shown to exhibit surge-like behavior in the past (Mayo, 1988; 1989). Visual inspection of imagery reveals that moraine patterns on Valerie Glacier during the 1993 and 2000 displacement events show a similarity to those seen in 1986. Landsat images acquired before and after the 1986 dam of Russell Fjord (http://edc.usgs.gov/earthshots/slow/Hubbard/Hubbard) reveal

that a loop moraine was formed on a medial moraine separating two trunks of Valerie Glacier (Fig. 2.6). This also coincided with contortion of this moraine further up glacier near the junction with Hubbard Glacier. During the time frame of the 1993 and 2000 displacement events, this moraine exhibited similar behavior of looping near the terminus and contortion further up glacier. This may suggest that surge-type behavior on Valerie Glacier may originate from one specific branch. We do not speculate here on the details of Valerie Glacier's surge-like behavior. However, we interpret that the behavior seen in 1986 is of the same type as what we have observed in 1993 and 2000. Our data suggest that Valerie Glacier may undergo these pulses on a somewhat regular basis with a periodicity of several years rather than decades, as is the norm for surge type glaciers (Raymond, 1987). These pulses also appear weaker than a full-scale glacier surge (Meier and Post, 1969; Clarke, 1987, Harrison and Post, 2003).

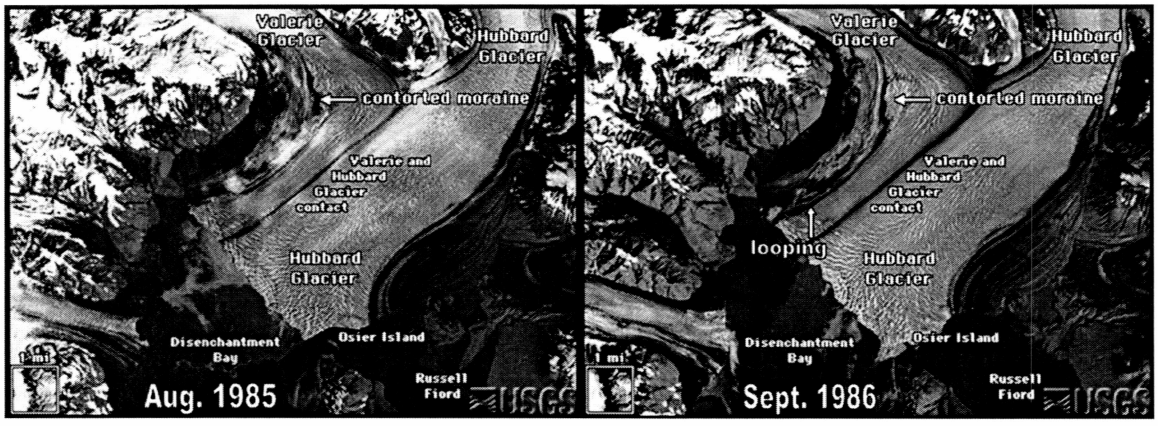

Figure 2.6. USGS Landsat images acquired before and after the 1986 damming of Russell Fjord reveal contorted and looped medial moraine on Valerie Glacier. Similar moraine behavior was observed in 1993 and 2000.

Figure 2.3a shows that the timing of the second displacement event coincided with an advance of the terminus. This section began to advance at an accelerated rate in 2000, which continued until the 2002 data gap. After 2002, the rate of advance slowed considerably. Figure 2.7 shows the terminus positions for Section A before 2000 compared to those after 2002. The position of the terminus fluctuated from year to year, but both the pre-2000 and post-2002 positions are tightly clustered. Between 2000 and 2002 the terminus advanced at an accelerated rate, but only onto land. In contrast, the

seaward portion of Section A showed little variation. The advance on land is consistent with the idea that a small "surge" of Valerie Glacier occurred at this time. We suggest that the section of the terminus ending in water was not able to advance significantly because of deeper water seaward of the submerged moraine crest. An advance over this crest would bring the glacier closer to flotation and calving would increase, forcing the terminus to calve back to a stable position. Where the ice terminates onto land, an increase in speed would advance the terminus at an accelerated rate. Figure 2.3a reveals that timing of the 1993 displacement event may also have coincided with a small change in terminus position, but temporal resolution of moraine positions does not allow for a definitive conclusion.

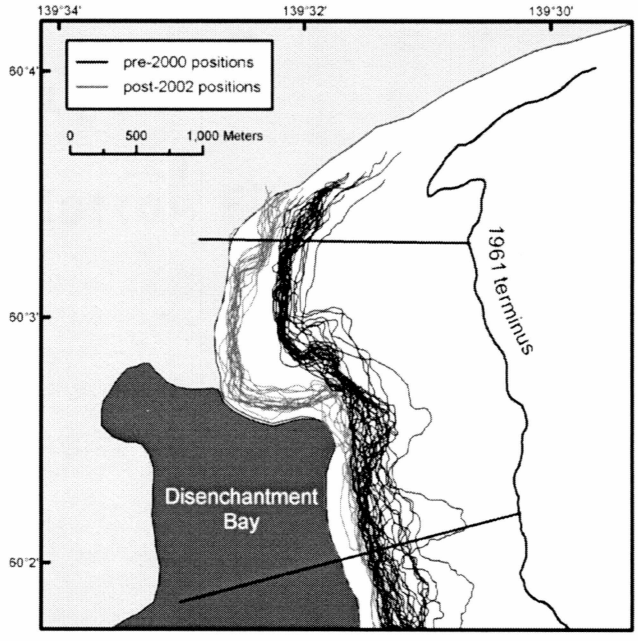

Figure 2.7. Terminus positions for the Valerie Glacier section (section A) before and after the 2000 medial moraine displacement event. Accelerated advance onto land suggests a surge-type event.

The sections of the terminus near Gilbert Point exhibited signs of having been affected by both medial moraine displacement events (Fig 2.3c,d). During the winter of 1993-94 Section C advanced 300 m. By October of 1994, Section C had calved back to approximately the same position that it held in the fall of both 1992 and 1993. Through

the winter of 1994-95, this section of the terminus advanced over 540 m to within 100 m of Gilbert Point. Once again, the ice had calved back to approximately the same fall position by October. These large scale fluctuations in terminus position occur simultaneously with the 1993 displacement event. Given the trend for 1992-1995, one might have expected that Hubbard Glacier would have closed off Russell Fjord in 1996, but it did not. Rather, the terminus near Gilbert Point returned to consistent behavior for the years 1996 to 2000. The moraine displacement event in 2000 appears to have affected this section of terminus in a similar fashion. Starting in the winter of 2001, Section C advanced 570 m and blocked the entrance to Russell Fjord in June of 2002 (Fig. 2.3c). This advance occurred simultaneously with the 2000 to 2002 displacement event. Section D also experienced accelerated advance in both 1994 as well as 2000, 2001, and 2002 (Fig. 2.3d). Given that the 1986 surge event and the 1993 and 2000 displacement events of Valerie Glacier all resulted in accelerated advance near Gilbert Point, it stands to reason that the flow relationship between Hubbard and Valerie Glaciers has a strong influence on terminus position in this region. This suggests that increased lateral ice flux into lower Hubbard Glacier caused by surges of Valerie Glacier may be a causal factor in the advances of terminus section C (Fig. 2.2) that block the entrance to Russell Fjord at Gilbert Point.

2.5.2 Ice Speed and Terminus Position

Based on photogrammetric analysis, Trabant and others (2003) reported center line ice velocities near the Hubbard Glacier terminus of 11.5 m d^{-1} in 2001. They also documented seasonal variations in surface ice speed of as much as 2 m d^{-1}. Centerline ice velocities near the terminus were 9.1 m d^{-1} from September 1988 through March 1989 (Krimmel, unp. data). Krimmel also measured a centerline velocity near the terminus of 13 m d^{-1} from April through May of 1989. The general trend was that speed increased throughout the winter with a maximum occurring in May and June. This speed maximum coincided with the time frame when the position of the terminus typically experienced advance (Fig. 2.3). During late summer, surface speed decreased, reaching a minimum

sometime between September and November. This minimum coincided with the time of typical seasonal terminus retreat (Fig. 2.3). If calving speed is held constant throughout the year, seasonal speed variations of 2 m d^{-1} could account for up to 360 m of seasonal terminus change according to Eqn. (2.1). The surface speed also varied spatially across the terminus. Typical observed speeds near the terminus were: Section A, ~4 m d^{-1}; Section B, ~13 m d^{-1}; Sections C and D, ~ 6 m d^{-1}; and Section E, less than 1 m d^{-1} (Krimmel, unp. data). While the seasonal variations in ice speed could explain the seasonal fluctuations in terminus positions, the spatial variation suggests that calving must also vary spatially to accommodate changing velocity. While the seasonal variations in ice speed could, in principle, explain the seasonal fluctuations in terminus positions, the spatial variations suggest that iceberg calving speed must also vary spatially across the terminus. Observations of other tidewater glaciers have shown that calving also varies seasonally. This strongly suggests that the observed seasonal changes in terminus position are functions of seasonal changes in both the forward component of the ice velocity and the calving velocity. Mechanical arguments can also be made to suggest that calving must also vary seasonally. Variations in velocity alone cannot account for the seasonality of the terminus position and other factors need to be considered.

2.5.3 Water Temperature and Terminus Position

Keeping in mind the difference in temporal resolution between the two datasets, there is an obvious correlation between seasonal fluctuations of terminus position and sea surface temperature. In a typical year, water temperatures increase 10 - 12 °C between April and August, and then decrease a similar amount between August and December (Fig. 2.5). In comparison, the terminus positions show a general trend of advance between October and May followed by retreat from May to the following October (Fig. 2.3).

Because our record of terminus positions shows a strong seasonal signal, it could be correlated to any other dataset exhibiting a seasonal signal. However, consideration of the influence of seawater temperature on terminus position comes from Q_c in Eqn. (2.2), which includes submarine melting. The model of submarine melting, and related calving,

proposed by Motyka and others (2003) is a function of both the temperature of incoming saline water and subglacial freshwater discharge. Upwelling of freshwater along the submerged ice face drives convection of saline ocean water. The resulting turbulent mixture melts glacier ice as it rises to the surface and forms an outflow plume of brackish water. High summer subglacial freshwater discharge and warm seawater result in greater submarine melting. The 15 m deep barrier moraine at the entrance to Yakutat Bay likely has a strong influence on the waters that enter Yakutat and Disenchantment Bays. This shallow moraine restricts inflow to the upper water column from the Gulf of Alaska. From April through August surface water temperatures increase, supplying warm saline water to the bay and eventually the terminal face, increasing submarine melting and iceberg calving. The summer increase in iceberg calving and submarine melting should increase the rate of retreat of the terminus (Eqns. 2.1, 2.2). Typically, we see such a retreat between May and October (Fig. 2.3). Evidence for "warm" seawater in Disenchantment Bay near the ice terminus during late August was reported by Motyka and Truffer (2007), who found that late-August water temperatures at 50 m depth averaged 9 - 10 °C. In contrast, April water temperatures at the same depth were 3 to 5 °C. The decrease in water temperature from August to December is typically followed by a period of relative cold stability. Low temperatures throughout December through March rarely vary by more than 1 °C; this combined with very low, or absent, freshwater discharge results in little to no calving, according to the convection model. Without strong calving at the terminus, the influx of ice into the terminus dominates Eqn. (2.2), driving the position of the terminus forward. Accordingly, our observations (Fig. 2.3) show that the terminus advances between October and May each year.

The model of convection-driven melting at the submarine ice face (Motyka and others, 2003) is strengthened by our observation of embayments opening in the terminal front along Disenchantment Bay. These embayments appear to have formed by localized increases in calving due to discharge streams emerging from beneath the terminus, which force convection and lead to submarine melting and undercutting of the face. The embayments only occurred along the section of the terminus bounded by Disenchantment

Bay, primarily in the western half of Section B (Fig. 2.2). The embayment locations did shift from year to year, indicating that the subglacial hydrological system changed with time. These openings were only observed in summer or fall and vanished by winter when the terminal face once again retained a relatively uniform geometry. Increased freshwater discharge at the terminus during the summers drove fjord seawater convection, drawing warm saline waters to the calving front. We note that these embayments occurred only in mid-late summer, a time when subglacial freshwater discharge was at its peak from surface melt on the glacier. This period coincided with a time when sea surface temperatures were at their seasonal high (Fig. 2.5). Therefore, the increased convection occurred at a time when the warmest saline water existed at the calving front. Motyka and others (2003) showed that submarine melting in late summer at LeConte Glacier contributed 57% of the estimated total ice loss at the terminus. The fact that we observed enhancement occurring exclusively in the summer can help explain the seasonal variations at the terminus of Hubbard Glacier.

While large seasonal fluctuations are seen in both terminus position and sea surface temperature, a correlation between annual changes in sea surface temperature and terminus position is not apparent. One might expect that unusually warm summer water temperatures, such as those seen in 2004, would result in relatively high calving rates, and therefore a larger seasonal retreat compared to other years. Similarly, relatively warm winter water temperatures, such as those seen in 1997-98, might be expected to cause increased calving and result in a relatively small seasonal advance. These correlations at the terminus did not occur consistently. For example, the Disenchantment Bay section of the terminus (Fig. 2.3b) exhibited a large winter advance in 2001-02 corresponding to relatively low water temperatures (Fig. 2.5). However, the winter of 1996-97 showed a similar water temperature record but the terminus experienced average advance during this time period. These inconsistencies can be found throughout the SST record. This lack of correlation may, in part, be explained by the relatively small change in temperature seen from year to year (1 - 2 °C) compared to the seasonal variations (10 - 12 °C). Also note that there is a 0.5 °C uncertainty in the temperature data. Changes in the influx of ice

at the terminus may also be playing a role. It is likely that, while water temperature plays a vital role in calving, a complex combination of many factors must be used to explain the fluctuations in terminus position.

2.5.4 Water Depth and Terminus Position

Water depth at the terminus has been shown to be a key factor in calving of tidewater glaciers (Post, 1975; Brown and others, 1982; Meier and Post, 1987; Van der Veen, 1996; Motyka and others, 2003). According to Brown and others (1982), the annual average calving speed is linearly dependent on the average water depth at the terminus. The model proposed by Van der Veen (2002) uses a height-above-buoyancy criterion for terminus position. Both models require knowledge of water depth; at an advancing glacier, such as Hubbard, the bed geometry is highly variable with time due to the ever-changing moraine crest. While the 60 - 100 m ice cliff places the terminus well above flotation, Van der Veen's model may be applicable as the terminus advances past the anchoring moraine into deeper waters. In such a situation, this model would require the glacier to calve back to a position where the water depth satisfies the height-above-buoyancy criteria. This provides a mechanism to explain how changes in ice speed are accommodated by similar changes in calving speed. However, application of this model would require an accurate knowledge of water depth at the terminus as a function of time. Unfortunately, repeat measurements of water depth along the calving front of a glacier like Hubbard would be both dangerous and expensive.

Tidal currents, water temperature, and water depth have been shown to be important factors in controlling the position of Section C of the terminus (Motyka and Truffer, 2007). Large tidal currents, combined with freshwater subglacial discharge, lead to fjord convection and increase submarine melting and hence calving, which controls terminus position. Motyka and Truffer (2007) have shown how water depth in the gap near Gilbert Point has changed with time. A steady accumulation of sediments over time, decreasing water depth, is contrasted by the 1986 and 2002 outburst floods which rapidly increased water depth. They suggest that water depth within this gap must be sufficiently shallow

for the closure of Russell Fjord. We propose that the combination of water depth and pulses in the speed of Valerie Glacier are essential factors in contributing to the periodic closure of Russell Fjord. This was the case in 1986 when sufficiently shallow waters and a surge of Valerie Glacier resulted in closure. The 1993 event exhibited similar behavior and caused the terminus near Gilbert Point to advance an abnormally large distance for two years in a row (Fig. 2.3). However, each summer the terminus calved back to approximately the same position. During this period, the water depth in the Gilbert Point gap was still relatively deep as a result of the 1986 outburst flood. Not enough time had passed for the accumulation of sediment to yield sufficiently shallow water. A combination of insufficiently shallow waters, warm seawater, and strong tidal currents forced Section C to calve back to a stable position. By 2002, after 8 more years of sediment accumulation, the water depth near Gilbert Point was shallow to inhibit calving and submarine melting fueled by tidal currents. At this time a pulse from Valerie Glacier appears to have provided a sufficient increase in ice velocity at the terminus. This, combined with inhibited calving due to shallow water, caused closure at Gilbert Point. On average, spring terminus positions resulted in a ~300 m wide gap at Gilbert Point. A 200+ m displacement due to a pulse from Valerie Glacier may be sufficient for closure, provided shallow waters inhibit submarine melting and calving.

Surging of a much smaller tributary on the upper reaches of Hubbard Glacier was witnessed in 2000 (Keith Echelmeyer, pers. comm., February 2007). Although it is unlikely that this had any significant effect at the terminus, it is important to consider that surging of other, larger, tributaries could have similar effects as those seen from pulses of Valerie Glacier. Since most of the tributaries of Hubbard exist in perpetually snow covered areas, surging would be much more difficult to detect using SAR imagery.

2.5.5 Implications for Terminus Stability

One of the biggest unknowns concerning tidewater glaciers is the initiation of retreat. How far can a terminus retreat from its terminal moraine shoal before a catastrophic retreat is initiated? We observed seasonal retreats of the terminus of Hubbard Glacier as

large as 500 m, yet a full scale retreat was not initiated. In fact, just the opposite, after each large retreat the terminus advances to an even further down-fjord position by the following spring. Work on Columbia Glacier revealed similar seasonal variations in its terminus position (Krimmel 2001). From 1977-1982, Columbia Glacier experienced average retreats of ~300 m between early summer and late fall. However, the terminus only advanced about half of that distance through the following winters. Beginning in 1982, Columbia Glacier began its catastrophic retreat. During summers retreats averaged ~1000 m, sometimes up to 1500 m. Winter advances were less than half of this amount.

Just what are the differences between Hubbard and Columbia Glaciers that explain why Hubbard has not started an irreversible retreat? One primary difference is the extreme negative mass balances measured and mapped by Meier and others (1985) on lower Columbia Glacier. They showed that the lower glacier was losing mass from ablation and flow to the calving front much more rapidly than it could be replaced by flow from up-glacier. These behaviors are not characteristic of Hubbard Glacier, which has a large and relatively high-altitude accumulation area, a relatively small ablation area, and an accumulation area ratio (AAR) > 0.9. It should be noted, however, that this astonishingly high AAR becomes much lower when iceberg calving is taken into account as a form of ablation (i.e., mass loss). In addition, Hubbard Glacier (unlike Columbia Glacier) is not experiencing rapid surface lowering in its lower reaches. Rather, Trabant and others (2003) observed increasing surface elevations near the terminus of Hubbard Glacier.

The model proposed by Van der Veen (2002) relates calving speed to thickness change at the terminus. This raises the question as to whether a warming climate could reverse the thickening trend seen at the terminus of Hubbard Glacier; if so, could this result in a premature retreat? A more detailed comparison of Hubbard and Columbia Glaciers may help explain the physical controls on calving and the underlying question of tidewater glacier stability.

2.6 CONCLUSIONS

The entire terminus of Hubbard Glacier has advanced approximately 620 m from 1992 to 2006 at an average rate of 35 m a^{-1}. Superimposed on this steady advance are regular summer retreats and winter advances which average 150 m, and can be as high as 500 m. Changes in terminus position are caused by the difference between the forward component of the ice velocity and the calving velocity at the terminal face. Two potential mechanisms capable of producing these fluctuations are seasonal variations in ice velocity and seasonal variations in submarine melting at the calving face. The ice velocity at the terminus has been shown to vary seasonally and spatially. While seasonal variations in velocity may be large enough to account for the variations we have observed in terminus position, the spatial variation of velocity along the calving front suggests that a combination of changes in ice speed and calving rate control seasonal terminus positions. Examination of water temperature records revealed a seasonal variability of 10 - 12 °C. Summer increases in seawater temperature and evidence of summer increases in freshwater discharge combine to drive summer increases in ice loss at the terminus through calving and submarine melting. The relationship between water depth and calving also has implications for determining terminus position. Rate of terminus change is also a function of water depth at the position of the terminus. All three of these factors are acting to drive the seasonal fluctuations as well as the long-term advance of Hubbard Glacier.

Displacement of the medial moraine separating the main trunks of Hubbard and Valerie Glaciers (Fig. 2.2) resulted from changes in the ice flow of Valerie Glacier. In 1993 and 2000 pulses in the speed of Valerie Glacier (resembling small-scale surges) caused changes in terminus position. The 2000 event, and possibly the 1993 event, advanced the western end of the terminus onto land at an accelerated rate, indicating an increase in the velocity of Valerie Glacier. The timing of these displacement events has been shown to correlate with changes in terminus position of Sections C and D near Gilbert Point. Shallow waters in this area reduce submarine melting and calving, which tends to result in terminus advance. Continued accumulation of sediments in the gap

increases the probability of another closure because the calving rate is reduced. Pulses from Valerie Glacier are likely to accelerate the advance of terminus Section C and, if water depth is shallow, the gap will once again be blocked. For prediction of future closures, a successful monitoring program should include both bathymetric measurements in the gap between the calving terminus and Gilbert Point, and yearly assessments of medial moraine displacement.

We foresee two possible scenarios for future closures of Russell Fjord. In the first case, enough sediment accumulates near Gilbert Point to allow the terminus to advance and close the gap. In this situation the advance may or may not be facilitated by pulsing or surging of Valerie Glacier or another tributary glacier. This scenario is less likely to result in a permanent closure, though it is not unrealistic. Although a combination of tidal forces, warm saline water, and water depth have resulted in little or no advance of Section C, the steady advance across the rest of the terminus must eventually force advance at Gilbert Point. In this second scenario, the terminus at Gilbert Point will be forced to "catch-up" to the rest of the terminus and block the entrance to Russell Fjord. This second scenario is more likely to eventually result in a long-term blockage of the entrance to Russell Fjord, accompanied by continuing advance of Hubbard Glacier into Disenchantment Bay and newly formed Russell Lake. However, the higher level of a dammed Russell Lake leaves the possibility of several more dam formations with subsequent outburst events, perhaps with slowly increasing dam stability (Motyka and Truffer, 2007).

2.7 ACKNOWLEDGEMENTS

We thank the NASA Solid Earth and Natural Hazards Program for supporting this work with grant NAG5-13760 (NRA-01-OES-05), the NASA Cryospheric Sciences Program for providing joint funding of this grant, and the Interdisciplinary Science in the NASA Earth Science Enterprise for providing support for this work with grant NNG04GH64G (NRA-03-OES-03). We thank Rudi Gens and Anupma Prakash for their assistance with satellite image processing; Anthony Arendt and Sandra Zirnheld for assistance with

analysis methods; and Keith Echelmeyer, Will Harrison, and Chris Larsen for discussions that improved the manuscript.

Bibliography

Arendt, A.A., K.A. Echelmeyer, W.D. Harrison, C.S. Lingle, and V.B. Valentine. 2002. Rapid wastage of Alaska glaciers and their contribution to rising sea level. *Science*, **297**(5580), 382-386.

Barclay, D.J., P.E. Calkin, and G.C. Wiles. 2001. Holocene history of Hubbard Glacier in Yakutat Bay and Russell Fiord, southern Alaska. *Geol. Soc. Am. Bull.*, **113**(3), 388-402.

Brown, C.S., M.F. Meier, and A. Post. 1982. Calving speed of Alaska tidewater glaciers, with application to Columbia Glacier. *U.S. Geol. Surv. Prof. Pap.* 1258-C.

Clarke, G.K.C. 1987. Fast glacier flow: ice streams, surging, and tidewater glaciers. *J. Geophys. Res.*, **92**(B9), 8835-8841.

Cowen, E.A., P.R. Carlson, and R.D. Powell. 1996. The marine record of the Russell Fjord outburst flood, Alaska, USA. *Ann. Glaciol.*, **22**, 194-200.

Davidson, G. 1903. *The Alaska boundary*. San Francisco, Alaska Packers Association.

Harrison, W.D. and A.S. Post. 2003. How much do we really know about glacier surging?. *Ann. Glaciol.*, **36**, 1-6.

Hunter, L.E. and R.D. Powell. 1998. Ice foot development at temperate tidewater margins in Alaska. *Geophys. Res. Ltrs.*, **25**(11), 1923-1926.

Jacobs, S.S., H.H. Helmer, C.S.M. Doake, A. Jenkins, and R.M. Frolich. 1992. Melting of ice shelves and the mass balance of Antarctica. *J. Glaciol.*, **38**(130), 375-387.

Krimmel, R.M. and B.H. Vaughn. 1987. Columbia Glacier, Alaska - Changes in velocity 1977-1986. *J. Geophys. Res.*, **92**(B9), 8961-8968.

Krimmel, R.M. 2001. Photogrammetric data set, 1957-2000, and bathymetric measurements for Columbia Glacier, Alaska. *U.S. Geol. Surv. Water-Res. Invest. Rep.* 01-4089.

Larsen, C.F., R.J. Motyka, A. Arendt, K.A. Echelmeyer, and P.E. Geissler. 2007. Glacier changes in southeast Alaska and northwest British Columbia and contribution to sea level rise. *J. Geophys. Res.*, **112**, F01007.

Mayo, L.R. 1988. Advance of Hubbard Glacier and closure of Russell Fiord, Alaska - Environmental effects and hazards in the Yakutat area. *In*: Galloway, J.P., and T.D. Hamilton, eds., Geologic studies in Alaska by the U.S. Geological Survey during 1987, *U.S. Geological Survey Circular 1016,* 4-16.

Mayo, L.R. 1989. Advance of Hubbard Glacier and 1986 outburst of Russell Fiord, Alaska, U.S.A. *Ann. Glaciol.*, **13**, 189-194.

Meier, M.F. and A. Post. 1969. What are glacier surges?. *Can. J. Earth Sci.* **6**(4 pt. 2), 807-817.

Meier, M F. and A. Post. 1987. Fast tidewater glaciers. *J. Geophys. Res.*, **92**(B9), 9051-9058.

Meier, M.F., L.A. Rasmussen, and D.S. Miller. 1985. Columbia Glacier in 1984: disintegration underway. *U.S. Geol. Surv. Open File Report* 85-81 (17 pp.).

Meier, M. *and 9 others*. 1994. Mechanical and hydrologic basis for the rapid motion of a large tidewater glacier. *J. Geophys. Res.*, **99**(B8), 15,219-15,229.

Mickelson, D.M., L.J. Acomb, and C.R. Bentley. 1981. Possible mechanism for the rapid advance and retreat of the Lake Michigan lobe between 13,000 and 11,000 years BP. (Abstract only) *Ann. Glaciol.*, **2**, 185-186.

Motyka, R.J. and J.E. Beget. 1996. Taku Glacier, Alaska, USA: Late Holocene history of a tidewater glacier. *Arct. Alp. Res.*, **28**(1), 42-51.

Motyka, R.J., L. Hunter, K.A. Echelmeyer, and C. Connor. 2003. Submarine melting at the terminus of a temperate tidewater glacier, LeConte Glacier, Alaska, U.S.A. *Ann. Glaciol.*, **36**, 57-65.

Motyka, R.J., M. Truffer, E.M. Kruiger, and A.K. Bucki. 2006. Rapid erosion of soft sediments by tidewater glacier advance: Taku Glacier, Alaska, USA. *Geophys. Res. Ltrs.*, **33**, L24504.

Motyka, R.J. and M. Truffer. 2007. Hubbard Glacier, Alaska: 2002 closure of Russell Fjord and implications for future dams. *in press*.

O'Neel, S., K.A. Echelmeyer, R.J. Motyka. 2001. Short-term flow dynamics of a retreating tidewater glacier: LeConte Glacier, Alaska, USA. *J. Glaciol.*, **47**(159), 567-578.

O'Neel, S., K.A. Echelmeyer, R.J. Motyka. 2003. Short-term variations in calving of a tidewater glacier: LeConte Glacier, Alaska.. *J. Glaciol.*, **49**(167), 587-598.

Pelto, M.S. and C.R. Warren. 1991. Relationship between tidewater glacier calving velocity and water depth at the calving front. *Ann. Glaciol.*, **15**, 115-118

Plafker, G. and D.J. Miller. 1958. Glacial features and surficial deposits of Malaspina District, Alaska. *U.S. Geol. Surv. Misc. Geol. Invest.* 1-271, map (scale 1:125,000).

Pollard, D. 1984. Some ice-age aspects of a calving ice-sheet model. *In*: Berger, A.L., J. Imbrie, J. Hays, G. Kukla, and B. Salzman, eds., *Milankovitch and climate, Part 2.* Dordrecht: Reidel Publ. Co., 541-564

Porter, S.C. 1989. Late Holocene fluctuations of the fjord glacier system in Icy Bay, Alaska, USA. *Arct. Alp. Res.*, **21**(4), 364-379.

Post, A. 1975. Preliminary hydrography and historic terminal changes of Columbia Glacier, Alaska. *U.S. Geol. Sur. Hydrol. Invest. Atlas* HA-559, 3 maps (scale 1:10,000).

Post, A. and R.J. Motyka. 1995. Taku and LeConte Glaciers, Alaska: calving-speed control of Late-Holocene asynchronous advances and retreats. *Phys. Geogr.*, **16**(1), 59-82.

Raymond, C.F. 1987. How do glaciers surge? A review. *J. Geophys. Res.*, **92**(B9), 9121-9134.

Reeh, N. 1994. Calving from Greenland glaciers: observations, balance estimates of calving rates, calving laws. *In*: Reeh, N., ed., *Workshop on the calving rate of West Greenland glaciers in response to climate change, Sept. 13-15, 1993*. Copenhagen, Danish Polar Center, 85-102.

Rignot, E. and P. Kanagaratnam. 2006. Changes in the velocity structure of the Greenland Ice Sheet. *Science,* **311**(5763), 986-990.

Sikonia, W.G. 1982. Finite-element glacier dynamics model applied to Columbia Glacier, Alaska. *U.S. Geol. Surv. Prof. Pap.* 1258-B.

Sohn, H., K.C. Jezek, and C.J. Van der Veen. 1998. Jakobshavn Glacier, West Greenland: 30 years of spaceborne observations. *Geophys. Res. Ltrs.*, **25**(14), 2699-2702.

Trabant, D.C., R.M. Krimmel, and A. Post. 1991. A preliminary forecast of the advance of Hubbard Glacier and its influence on Russell Fiord, Alaska. *U.S. Geol. Surv. Water-Res. Invest. Rep.* 90-4172.

Trabant, D.C., R.M. Krimmel, K.A. Echelmeyer, S.L. Zirnheld, and D.H. Elsberg. 2003. The slow advance of a calving glacier: Hubbard Glacier, Alaska, U.S.A. *Ann. Glaciol.* **36**, 45-50.

Walters, R.A., E.G. Josberger, and C.L. Driedger, 1988. Columbia Bay, Alaska: An "upside down" estuary. *Estuarine Coastal Sci.*, **26**(6), 607-617.

Warren, C.R., N.F. Glasser, S. Harrison, V. Winchester, A.R. Kerr, and A. Rivera. 1995. Characteristics of tide-water calving at Glaciar San Rafael, Chile. *J. Glaciol.*, **41**(138), 273-289.

Wiles, G.C., D.J. Barclay, and P.E. Calkin. 1999. Tree-ring-dated 'Little Ice Age' histories of maritime glaciers from western Prince William Sound, Alaska. *The Holocene.* **9**(2), 163-173.

Van der Veen, C.J. 1996. Tidewater calving. *J. Glaciol.*, **42**(141), 375-385.

Van der Veen, C.J. 1999. *Fundamentals of glacier dynamics*. Rotterdam, A.A. Balkema.

Van der Veen, C.J. 2002. Calving glaciers. *Progress in Phys. Geogr.*, **26**(1), 96-122.

Chapter 3

General Conclusions

Observations of lower Hubbard Glacier, Alaska, reveal that a complex combination of ice speed and calving rate controls terminus position. During the 15 year period of this study, Hubbard Glacier has steadily advanced at a mean rate of 35 m a^{-1}. Superimposed on this advance are summer retreats alternating with winter re-advances of up to 500 m. Observations of the medial moraine separating Hubbard and Valerie Glaciers reveal that instabilities in the flow relationship between these two glaciers may occur with a periodicity of several years, supporting the idea that Valerie Glacier exhibits surge behavior.

The waters of Yakutat and Disenchantment Bays show a seasonal variability of 10 - 12 °C. Increased summer seawater temperature and evidence of summer increases in freshwater discharge combine to drive summer increases in ice loss at the terminus through calving and submarine melting. The relationship between water depth and calving also has implications for determining terminus position. These factors drive the observed long-term advance and seasonal fluctuations of the calving terminus of Hubbard Glacier. Timing of "mini-surges" of Valerie Glacier suggests that these events influence the position of sections of the terminus. In 1986 and 2002, pulses from Valerie Glacier occurred simultaneously with periods of sufficiently shallow waters near Gilbert Point, the combined effect being the damming of Russell Fjord. Therefore, programs to monitor possible future closures of Russell Fjord should include both bathymetric measurements, as well as a method of monitoring for pulses in the speed of Valerie Glacier.

To better understand tidewater glacier dynamics and tidewater calving, near simultaneous measurements of seasonal ice speed, calving rate, water temperature, and bathymetry, should be combined with a record of terminus positions. Evidence from this and other studies demonstrate that a combination of these factors determine terminus position of a tidewater glacier. Hence the calving rate, the position of the terminus, the area-average surface elevation rate on the lower glacier, and the mass balance of the

whole glacier system, would be likely to yield significantly improved knowledge and understanding of the tidewater Hubbard Glacier.

Appendix A

Table of Satellite Imagery Used

Date	Platform	Granule ID
01-Feb-92	ERS-1	E1_02863_STD_300
06-May-92	ERS-1	E1_04224_STD_300
03-Aug-92	ERS-1	E1_05498_STD_300
28-Oct-92	ERS-1	E1_06729_STD_300
25-Jan-93	ERS-1	E1_08003_STD_300
10-May-93	ERS-1	E1_09506_STD_299
04-Aug-93	ERS-1	E1_10737_STD_300
13-Oct-93	ERS-1	E1_11739_STD_300
02-Feb-94	ERS-1	E1_13343_STD_300
16-May-94	ERS-1	E1_14820_STD_299
01-Aug-94	ERS-1	E1_15925_STD_300
14-Oct-94	ERS-1	E1_16987_STD_300
02-Feb-95	ERS-1	E1_18580_STD_300
03-May-95	ERS-1	E1_19870_STD_299
28-Jul-95	ERS-1	E1_21101_STD_300
25-Oct-95	ERS-1	E1_22375_STD_299
07-Feb-96	ERS-1	E1_23878_STD_299
03-May-96	ERS-1	E1_25109_STD_300
17-Aug-96	ERS-2	E2_06939_STD_300
26-Oct-96	ERS-2	E2_07941_STD_300
27-Feb-97	ERS-2	E2_09716_STD_300
28-Jun-97	ERS-2	E2_11448_STD_300
12-Jul-97	RADARSAT-1	R1_08805_ST2_300
25-Sep-97	ERS-2	E2_12722_STD_300
30-Oct-97	ERS-2	E2_13223_STD_300
24-Jan-98	ERS-2	E2_14454_STD_300
28-May-98	ERS-2	E2_16229_STD_300
06-Aug-98	ERS-2	E2_17231_STD_300
26-Sep-98	ERS-2	E2_17961_STD_300
08-Feb-99	RADARSAT-1	R1_17037_ST2_300
24-Apr-99	ERS-2	E2_20967_STD_300
07-Aug-99	ERS-2	E2_22470_STD_300
06-Oct-99	RADARSAT-1	R1_20467_ST2_300
03-Feb-00	RADARSAT-1	R1_22182_STD_300

09-May-00	RADARSAT-1	R1_23554_ST2_300
05-Jun-00	Landsat ETM+	LE7062018000015750
20-Jul-00	RADARSAT-1	R1_24583_ST2_300
01-Oct-00	Landsat ETM+	LE7062018000030150
05-Apr-01	ASTER	04052001205827_12212003100329
08-Jun-01	Landsat ETM+	p062r018_7t20010608_z08
07-Jul-02	NMFS aerial photograph	
19-Sep-02	ERS-2	E2_38774_STD_300
24-Oct-02	ERS-2	E2_39275_STD_299
06-Feb-03	ERS-2	E2_40778_STD_300
18-May-03	RADARSAT-1	R1_39332_ST2_300
05-Aug-03	RADARSAT-1	R1_40461_ST3_300
06-Oct-03	RADARSAT-1	R1_41347_ST4_300
06-Feb-04	RADARSAT-1	R1_43105_ST2_300
09-May-04	RADARSAT-1	R1_44434_ST4_300
02-Aug-04	RADARSAT-1	R1_45649_ST1_300
13-Oct-04	RADARSAT-1	R1_46678_ST1_299
31-Jan-05	RADARSAT-1	R1_48250_ST2_300
17-May-05	RADARSAT-1	R1_49765_ST1_299
01-Aug-05	RADARSAT-1	R1_50851_ST4_300
22-Oct-05	RADARSAT-1	R1_52023_ST2_300
07-Feb-06	RADARSAT-1	R1_53559_FN1_150
19-Jun-06	RADARSAT-1	R1_55453_ST2_300
03-Aug-06	RADARSAT-1	R1_56096_ST4_301
20-Sep-06	RADARSAT-1	R1_56782_ST4_301

Appendix B

Detailed Methods and Suggestions

The following is a detailed description of the methods used for acquiring satellite imagery; geocoding and co-registration of the images; and processing terminus and medial moraine position data. This is provided so that future work may be conducted using the same methods which were used for this study. Suggestions for improvements are also included throughout. The terminus position data process description provided is for use of ESRI's ArcGIS 9.2, however the process uses standard tools which are available with most image processing software.

Obtaining Satellite Imagery

SAR imagery is obtained through ASF using data credits supplied by NASA and ASF. Images are ordered through the ASF website (http://www.asf.alaska.edu/) by selecting "Get SAR DATA" from the main page and then by selecting "Order L1 Data Products" which will redirect you to NASA's Earth Observing System (EOS) Data Gateway.

EOS Data Gateway

- You must enter the data gateway as a guest. A number of tabs appear in the toolbar to the left, you will be working through the "Search and Order" tabs to obtain images. Starting with User Preferences you must fill in your contact address and your affiliation. To obtain images you must have ASF data credits obtained through a short proposal process. The data credits have an ASF Data Access Key associated with them which must be supplied to this page under your affiliation. Upon input of profile information you must select "Update User Profile". You have an option to "Save Prefs" which can create a *.dat file which can be used at another time by choosing to restore user preferences from a file.
- Then under the Search Creation tab you must select the option of Choose Data Sets "By Categories/Attributes" and then select DATA SET and click the "Choose Keywords for >>" button. Here you will choose the ASF Filter and select "Apply".

Then you will select the appropriate data sets (multiple data sets can be selected by holding the Ctrl button). The data sets which apply to this study are:

ERS-1 SAR IMAGES – FULL RES

ERS-2 SAR IMAGES – FULL RES

RADARSAT-1 FINE RESOLUTION IMAGES – FULL RES

RADARSAT-1 STANDARD BEAM IMAGES – FULL RES

Choosing these data sets and selecting OK will bring you back to the previous page which should now have these data sets selected. The Data Search Type remains selected at "Primary Data Search". Choosing a search area can be done using a number of options. The "Orthographic (Java)" option has proven to be easy as it allows you to select a rectangle as a search area. Whichever option is used here, the search area should only contain the terminus region of Hubbard Glacier. Then you must choose the date/time range within which you wish to obtain imagery. Additional options can also be changed but have typically been left at the default setting. You are now ready to "Start Search".

- This process may take a few minutes to complete and upon completion you will be redirected to the Results: Data Set tab. Here you will select all the datasets you wish to browse and then select "List data granules". For images after 2006 the ERS-1 and 2 datasets are not available as these satellites are no longer operational but they may be appropriate for earlier images.
- This will bring you to the Results: Granule tab and here you will browse and choose which image or images you want to order. The previous methodology in choosing an image was to obtain 4 images each year, once per season, at approximately the same time each year. However, this may result in significant error which can be corrected for by choosing images which are exact repeat orbits and obtaining an appropriate number of images (at least 4) spaced evenly throughout the year to establish a seasonal cycle. Repeat images within a dataset can be identified by their Data Granule ID. For Radarsat images, the first two characters represent that it is a Radarsat image, the next set of numbers represent the acquisition time, the next characters represent

the beam type (standard or fine resolution), and the final three numbers represent an image number. It is likely that fine resolution images will be available with adequate timing, if so, these images should be the first choice as they have 7.5 m resolution. For any two fine resolution (or standard beam) images to be exact repeats the numbers representing data acquisition time must be separated by an even multiple of 343. This will ensure the images are acquired some multiple of 24 days apart. By selecting an image and clicking "Show map coverage" you can see a footprint of where the image is located. The idea is to find an image which was acquired at the approximate time you are looking for and to make sure that it has an appropriate image footprint. Then any consecutive images obtained should be exact repeat orbits of this initial image. As long as the image is an exact repeat the image footprint will be the same. Once you have decided which images you wish to order, you need to select them and click "Add selections to cart".

- This will direct you to the Shopping Cart tab where you can view the images you have selected and "Choose Options" for ordering. Here you will choose the media format which you want to receive the data on. Regardless of which media format chosen, you must select the option of "NORMAL" Data Format. Choosing NORMAL CD or NORMAL DVDR will result in ASF contacting you to pick up your order when it is complete (about a week). There is also an option for FTP which I believe you would want as the CEOS SAR FILE and this option may be quicker but has never been used during this study. You may choose to apply these options to only this image or to all images within a data set and then select OK. Once you have chosen the options for all of your images you can click "Go to Step 2: Order Form" where you can supply contact information and review and submit your order.

Geocoding

Geocoding of images is done using ASF's Convert tool which is available at the ASF website by selecting "Get SAR TOOLS". As of April 2007 the most current version is

Convert 3.0.2. It is important to stay up to date on the latest versions of this tool as they become available through the ASF website as there may exists corrections or improvements which could enhance the geocoding process.

ASF Convert Tool 3.0.2

- This tool is set up with tabs with which to navigate through all of the options. The Import tab allows you to select what form of input will be used. In this case the data is CEOS (Level 1). There is also an option here which allows intermediate files to be saved if you find reason to view these files later.
- The Radiometry tab changes the radiometric data type. This is not much of a concern for this study and has been left at the default value of Amplitude.
- The DEM tab is used for terrain correction. An attempt was made to use terrain correction for this study, but problems existed relating to masking of ice and water. Terrain correction requires accurate knowledge of the current terrain at time of image acquisition. Due to the fact that the terminus position is changing, this is not feasible. It may be possible to use a mask to perform terrain correction in the future, however this did not work during the course of this study and so was not further pursued.
- Under the Geocode tab you must select to geocode and choose the appropriate projection. For this study I have used UTM with the WGS84 Datum. The zone will be selected automatically but can be input as 7N. The resample method to use is Bilinear.
- Under the Export tab you must select GeoTIFF (.tif) as the format. For this study, nothing is gained by outputting the images in floating point format so you can select the "Output data in byte format (instead of floating point)" option to reduce file size. In this case the Sample mapping method used is Statistical 2 Sigma.
- After selection of all the options, a summary can be viewed in the right hand corner and you can select the files you would like to convert. The files come from ASF as .D and .L files. You can "Browse" to add files and supply the location of all of the .D files which you want to convert. Here you can also change the output directory and supply a Naming Scheme (prefix or suffix) to all of the output data. Once you have

supplied the images and selected all of the options you can start the process by clicking "Execute". This process takes roughly 15-30 minutes.

Co-registration

After all of the images were geocoded, examinations of the images showed that there were still co-registration issues. To determine whether an image is properly co-registered it needs to be compared to a reference image. In this study the reference image used was a Radarsat-1 Fine Resolution image from February 7th, 2006. I have included this image on the supplement DVD and it also appears on the UAF Glaciology lab network. You can use this image to digitize the coastline around Gilbert Point and overlay this digitization on each new image to see how well they compare. If the coastline doesn't line up then a horizontal translation is likely needed to shift the new image to the same reference frame as the February 2006 image.

Image Shifting

- The idea behind shifting an image is to find what amount of translation is needed in both x and y directions to result in the shoreline near Gilbert Point to lineup in both the new and reference image. The shoreline may change with time due to erosion so there does not exist a single point which can be confidently compared and result in a value of offset for x and y. What I have done is to open a new ArcMap document and add the reference image and any images which need shifting to this document. While viewing the reference image only, I draw a line along the entire shoreline near Gilbert Point from near Haenke Island up and around to similar latitude on the Russell Fjord side of Gilbert Point. I have also marked the outline of Haenke Island for this process. Since these outlines represent lines, and not individual points, it is also necessary to digitize a single point in the vicinity of these outlines. This single point doesn't have to correspond to any feature in the image; you merely need to record the UTM coordinates of this point. Once you have drawn an outline corresponding to the shoreline in the reference image and marked and recorded a reference point, you will

then view these outlines along with an image which needs to be shifted. The outlines should not align with the shoreline in this image. You will select the outlines and the reference point and move them simultaneously by hand until the outlines match the shoreline in the image to be shifted. You must then record the new UTM coordinates for the reference point and then use the "undo" button to move the outlines and point back to their original position which matches the reference image.

- Using the difference in recorded UTM coordinates of the reference point, the image is shifted by this amount. This is done using the "Shift" tool from the ArcToolbox which is located under Data Management Tools>Projections and Transformations>Raster. Use the image to be shifted as the input, create a name for the new, shifted image, and input the translation amount for both X and Y. The new image should be viewed along with the reference image to be certain that they line up properly.

Image Processing

Now that your image has been geocoded and coregistered, it is ready to be processed in order to obtain a terminus position and medial moraine datum. It has been found to be useful to crop the images to an area of interest in order to work with smaller file sizes. Any area of interest will work as long as it includes the terminus and medial moraine, however the boundary used in this study has been included as a shapefile entitled "boundary" (supplement DVD and UAF Glaciology network). You will also find the file "term_1961_baseline" which contains the 1961 terminus and the baselines separating the 5 terminus sections. All of the GIS files included are shapefiles so that they may be used across platforms, however in this study the files were features used within a geodatabase. In this respect, the instructions given here are for ArcGIS feature class files.

Terminus Positions

- If using ArcGIS, the first step is to create a Personal Geodatabase and a Feature Dataset to store the terminus position features. The Dataset should be created with a

UTM WGS84 projection. For each image, a line feature class (or shapefile) is created; this will be the digitized terminus. The naming scheme used in this study for these files is "term_YYYY_MM", where YYYY is the year and MM is the month.

- The feature class (or shapefile) can now be opened in ArcMap along with the corresponding image. (If not using ArcGIS, the end result is to obtain a shapefile with data points for the digitized terminus for the image) Under the Editor tab, choose to "Start Editing" and select the feature class you want to edit. Under "Task" choose to "Create New Feature" and use the pencil tool to select points along the terminus. It has been found that a zoom level of 1:9,000 works the best, although zooming in and out as you proceed helps to ensure you are following the terminus. After the terminus is digitized such that it extends beyond the eastern and western boundaries of the 1961 baseline, choose to save and stop editing.
- Use the ArcToolbox to create polygons from the 1961 baseline and the newly digitized terminus file. The tool used is "Feature to Polygon" located under Data Management Tools>Features. The input features should be "term_1961_baseline" and the feature class you just created. The naming scheme for the output feature is "term_YYYY_MM_poly" where YYYY is the year and MM is the month.
- The result is 5 polygons which represent each of the sections of the terminus. Using the provided spreadsheet of terminus position data ("Hubbard Terminus advance since 1961"), create a new line and insert the date of image and area of each polygon. These areas can then be divided by the given width to determine width-averaged linear advance since 1961 for each section.

Medial Moraine Positions

- Create a feature class (or shapefile) to store the medial moraine position, the naming scheme is "med_YYYY_MM" where YYYY is the year and MM is the month.
- Digitize the center of the medial moraine in the same manner as the terminus positions.

- Using the provided shapefile entitled "med_baseline" and the digitized moraine position, use the tool "Feature to Polygon" to create a polygon as in the terminus positions.
- The area of this polygon is recorded in the provided spreadsheet "Medial Moraine Movement" and divided by the given length resulting in a value of offset from reference baseline averaged over the length of the medial moraine.